Eur. Phys. J. A **14**, 459–468 (2002)
DOI 10.1140/epja/i2002-10028-6

THE EUROPEAN PHYSICAL JOURNAL A

A model for fragment excitation and kinetic energy in nuclear fission

H.R. Faust[a]

Institut Laue-Langevin, BP 156 F-38042 Grenoble, Cedex 9, France

Received: 14 February 2002 / Revised version: 25 April 2002
Communicated by P. Schuck

Abstract. We present a model which allows for the calculation of fragment excitation and kinetic energy in nuclear fission. The model assumes that fission products are excited independently according to an exponential distribution function, which depends on the Q-value of the reaction and the level density parameter in the single fragment. We develop the model description and compare the results for different fissioning systems from actinium to fermium, and for different compound reactions, namely spontaneous fission, fission following thermal neutron capture, and high-energetic reactions with experimental data.

PACS. 24.75.+i General properties of fission – 25.85.Ec Neutron-induced fission – 25.85.Ca Spontaneous fission

1 Introduction

The model for fragment excitation in nuclear fission developed below is based on two axioms. The first one is that at the scission point, the excitation of the single fragment is described by an exponential with a mean energy of $\langle E^* \rangle = a \cdot (\bar{f}Q)^2$. Here a and Q are the level density parameter of the fragment and the Q-value of the reaction, respectively. The constant $\bar{f}$ connects fragment excitation and Q-value. The second axiom of the model is that both fragments are excited independently.

We will show that from the two axioms the whole energetics of the fission process is derived, and the equations for the calculation of mean total excitation energy, mean total kinetic and mean single-fragment kinetic energies can be given. In order to account for a maximum value of excitation in fission a cut-off parameter is introduced, which forces the exponential function describing single-fragment excitation to go to zero at high excitation energies. Whereas the cut-off parameter has little influence on mean values of the excitation and kinetic energies, it drastically reduces the variances of the distributions.

2 Excitation energy in spontaneous fission

The first axiom leads to the following expression for the excitation function for the two fragments in spontaneous fission:

$$\Phi(E^*_{1,2}) = N_0 \cdot \exp\left(-\frac{E^*_{1,2}}{a_{1,2}(\bar{f}Q)^2}\right) , \qquad (1)$$

where $a_{1,2}$ are the level density parameters for fragment 1 and 2, respectively. The reaction Q-value is calculated from the mass excesses Δ of the nuclei involved:

$$Q = \Delta_{\mathrm{CN}} - (\Delta_{f1} + \Delta_{f2}) . \qquad (2)$$

Mass excesses are taken from the compilation of the experimental data of Wapstra *et al.* [1] and from the calculations of Möller and Nix [2], when no experimental data exist. CN, f_1 and f_2 stand for the compound nucleus and the fragments, respectively.

The second axiom requires that the excitation of both fragments proceeds independently. The excitation of the combined system is found by inspecting the result of a simple Monte Carlo calculation. Here, four random numbers are chosen for E^*_1, E^*_2, $\Phi(E^*_1)$ and $\Phi(E^*_2)$. Whenever the combination of the 4 numbers falls into the distributions, eq. (1), the event is sorted into the spectrum of the total excitation energy $\mathrm{TXE} = E^*_1 + E^*_2$. This is shown in the upper part of fig. 1.

From the picture the TXE distribution function is easily guessed. It appears that, if the two fragments are excited independently according to eq. (1), the distribution function for the excitation of the total system can be approximated by

$$\Phi(\mathrm{TXE}) = N_0 \cdot \mathrm{TXE} \cdot \exp\left(-\frac{\mathrm{TXE}}{\frac{a_1+a_2}{2}(\bar{f}Q)^2}\right) . \qquad (3)$$

The last equation, in fact, is strictly valid only for $a_1 = a_2$, when totally independent excitation is required. If $a_1 \neq a_2$ the covariance, which can be calculated from the individual distributions, does not vanish, see sect. 7.

[a] e-mail: faust@ill.fr

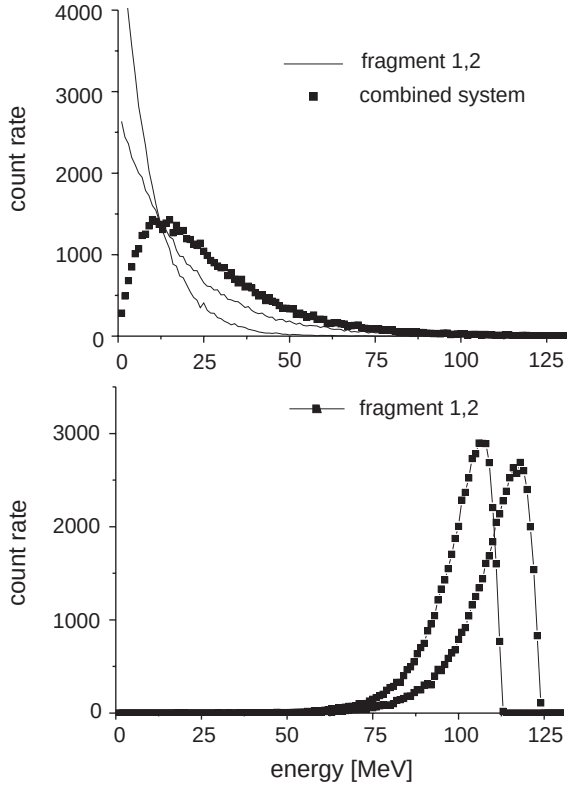

Fig. 1. Result of the Monte Carlo simulation. The following parameters for mass A, nuclear charge Z and level density parameter a were used: $A_1 = 120$, $Z_1 = 48$, $a_1 = 16.0$, $A_2 = 132$, $Z_2 = 50$, $a_2 = 8.0$. These values correspond to a mass split in ^{252}Cf(sf) with a Q-value of $Q = 236.6\,\mathrm{MeV}$. The upper part of the figure shows the excitation functions of the fragments and the distribution function for TXE. The lower part shows the distribution functions which follow for the kinetic energies.

For the fission reactions of the actinides, however, this covariance is always small.

The normalization constants for the distributions eq. (1) and eq. (3) are obtained by integration

$$N_0(E^*) = \frac{1}{a_{1,2}(\bar{f}Q)^2}\,, \tag{4}$$

$$N_0(\mathrm{TXE}) = \frac{2}{(a_1+a_2)^2}\frac{1}{(\bar{f}Q)^2}\,. \tag{5}$$

Also the mean values of the distributions can immediately be obtained by evaluating the following expression:

$$\langle x\rangle = \frac{\int \Phi(x)\cdot x}{\int \Phi(x)} \tag{6}$$

leading to

$$\langle E^*_{1,2}\rangle = a_{1,2}(\bar{f}Q)^2\,, \tag{7}$$

as required by axiom 1. For the mean of the total excitation energy, we get

$$\langle \mathrm{TXE}\rangle = (a_1+a_2)\cdot(\bar{f}Q)^2\,. \tag{8}$$

3 Kinetic energies

Kinetic energy in nuclear fission is the remaining part, when the excitation energy is subtracted from the Q-value for a given mass split. The total kinetic-energy distribution is therefore the mirror image of the TXE distribution. The distribution function is

$$\Phi(\mathrm{TKE}) = N_0\cdot(Q-\mathrm{TKE})\cdot\exp\left(-\frac{(Q-\mathrm{TKE})}{\frac{a_1+a_2}{2}(\bar{f}Q)^2}\right)\,. \tag{9}$$

The mean value of the TKE distribution is obtained by

$$\langle \mathrm{TKE}\rangle = Q - \langle \mathrm{TXE}\rangle\,. \tag{10}$$

Past the scission point only the long-range Coulomb force acts on the fragments, and accelerates them to the kinetic energies $E^{1,2}_{\mathrm{kin}}$. The fragments will share the total kinetic energy according to the momentum and energy conservation law. From the momentum law $A_1v_1 = A_2v_2$ and the expression for the kinetic energies $E = \frac{1}{2}Av^2$, we get

$$\frac{E^1_{\mathrm{kin}}}{E^2_{\mathrm{kin}}} = \frac{A_2}{A_1}\,. \tag{11}$$

The kinetic energy is distributed according to the inverse ratio of the fragment masses. The above features were introduced into the Monte Carlo program and the result is shown in the lower part of fig. 1. The evaluation of the analytical expression for the single-fragment kinetic energies leads to the (non-normalized) distribution function

$$f^{(i)}(E_{\mathrm{kin}}) = (Q-\frac{E_{\mathrm{kin}}}{\tilde{c}})\cdot\exp\left(\frac{-(Q-\frac{E_{\mathrm{kin}}}{\tilde{c}})}{\frac{(a_1+a_2)}{2}(\bar{f}Q)^2}\right)\,. \tag{12}$$

The index i stands for fragments 1 and 2, respectively, the constant $\tilde{c}$ depends on the fragment masses A_{L} and A_{H} in the binary fission process

$$\tilde{c}_{\mathrm{L}} = \frac{A_{\mathrm{H}}}{(A_{\mathrm{L}}+A_{\mathrm{H}})} \tag{13}$$

for the light-fragment distribution, and

$$\tilde{c}_{\mathrm{H}} = \frac{A_{\mathrm{L}}}{(A_{\mathrm{L}}+A_{\mathrm{H}})} \tag{14}$$

for the distribution function of the heavy fragment. The function (12) has a crossing at zero and becomes negative at $\left(Q-\frac{E_{\mathrm{kin}}}{\tilde{c}}\right) = 0$. The negative region is non-physical and has to be discarded in the calculation of the mean and the variance of the kinetic-energy distribution of the fragments. Inspecting fig. 1 shows, that that the shape of the kinetic-energy distribution is asymmetric, with a large tail to lower energies. This asymmetry of the shape comes from the asymmetry of the shape for Φ(TXE) and consequently Φ(TKE), which is, however, strongly modified by the requirement of energy and momentum conservation, when TKE is distributed between the fragments.

Mean kinetic-energy values are calculated using the analytical expressions of eq. (12). In the integration the upper limit of the integral is

$$x_0^{\mathrm{H}} = \left(\frac{A_{\mathrm{L}}}{A_{\mathrm{L}} + A_{\mathrm{H}}}\right) \cdot Q \tag{15}$$

for the heavy fragment and

$$x_0^{\mathrm{L}} = \left(\frac{A_{\mathrm{H}}}{A_{\mathrm{L}} + A_{\mathrm{H}}}\right) \cdot Q \tag{16}$$

for the light fragment.

All integrals which are needed to calculate mean and variances are of the form $\int x^m e^{ax} \mathrm{d}x$ and can be evaluated using recurrence relations, see [3].

With the foregoing expressions all distributions of single-fragment and total excitation energy and single-fragment and total kinetic energy for any spontaneous-fission process and any mass and charge split may be computed.

4 Fission induced by a reaction

If the fission process is induced by particles or γ-rays, the excitation energy due to the reaction with the projectile has to be taken into account. This part of the excitation has to be added at the compound-nucleus stage. We assume that the compound system gets to a common temperature and that subsequently the energy is shared between the fragments. With the known relationship from the statistical model, which connects excitation energy E and nuclear temperature kT in a compound nucleus, we have $E_1 = a_1 kT^2$ and $E_2 = a_2 kT^2$. Therefore, external excitation energy is shared between the fragments according to their level density parameter. The density distribution for single-fragment excitation and TXE becomes

$$\Phi(E_1^*) = N_0 \cdot \exp\left(-\frac{E_1^*}{a_1 \cdot (\bar{f}Q)^2 + \frac{a_1 \cdot \epsilon_{\mathrm{c}}}{(a_1+a_2)}}\right), \tag{17}$$

$$\Phi(E_2^*) = N_0 \cdot \exp\left(-\frac{E_2^*}{a_2 \cdot (\bar{f}Q)^2 + \frac{a_2 \cdot \epsilon_{\mathrm{c}}}{(a_1+a_2)}}\right), \tag{18}$$

$$\Phi(\mathrm{TXE}) = N_0 \cdot \mathrm{TXE} \cdot \exp\left(-\frac{\mathrm{TXE}}{\frac{a_1+a_2}{2}(\bar{f}Q)^2 + \frac{\epsilon_{\mathrm{c}}}{2}}\right), \tag{19}$$

with ϵ_{c} as the external excitation energy brought into the compound system. The mean values become

$$\langle E_1^* \rangle = a_1 (\bar{f}Q)^2 + \frac{a_1 \cdot \epsilon_{\mathrm{c}}}{(a_1 + a_2)}, \tag{20}$$

$$\langle E_2^* \rangle = a_2 (\bar{f}Q)^2 + \frac{a_2 \cdot \epsilon_{\mathrm{c}}}{(a_1 + a_2)}, \tag{21}$$

$$\langle \mathrm{TXE} \rangle = (a_1 + a_2) \cdot (\bar{f}Q)^2 + \epsilon_{\mathrm{c}}, \tag{22}$$

$$\langle \mathrm{TKE} \rangle = Q_R - \langle \mathrm{TXE} \rangle, \tag{23}$$

with

$$Q_R = Q + \epsilon_{\mathrm{c}}. \tag{24}$$

The expressions for the kinetic-energy distributions also change in induced reactions:

$$f^{(i)}(E_{\mathrm{kin}}) = \left(Q_R - \frac{E_{\mathrm{kin}}}{\tilde{c}}\right) \cdot \exp\left(\frac{-(Q_R - \frac{E_{\mathrm{kin}}}{\tilde{c}})}{\frac{(a_1+a_2)}{2}\left[(\bar{f}Q)^2 + \frac{\epsilon_{\mathrm{c}}}{a_1+a_2}\right]}\right). \tag{25}$$

5 Temperatures

In spontaneous fission the mean excitation of the single fragment was taken to be

$$\langle E^* \rangle = a \cdot (\bar{f}Q)^2. \tag{26}$$

The statistical model gives the expression for the temperature of a nucleus with the mean excitation energy as

$$\langle E^* \rangle = a \cdot (kT)^2. \tag{27}$$

From the analogy we derive that the temperature of the single fragment at the end of the fission process is

$$kT = \bar{f}Q. \tag{28}$$

Temperature of the single fragment depends on the Q-value, and therefore on the specific mass split. For fission induced by a nuclear reaction the temperature of the single fragment becomes

$$kT = \sqrt{(\bar{f}Q)^2 + \frac{\epsilon_{\mathrm{c}}}{a_1 + a_2}}. \tag{29}$$

6 Mean neutron evaporation

Past the scission point the excited fragments will decay by neutron and gamma emission. A model which is expected to reproduce the internal excitation probability for fission products has to be tested not only via the calculation of kinetic energy, but also has to reproduce the neutron evaporation from the fragments. In particular the universality of the sawtooth neutron evaporation probability, which is observed for all compound systems must emerge. In order to calculate the mean neutron evaporation values $\langle M_\nu \rangle$ from fission products it is possible to use the approach given by Stwertka [4]:

$$\langle M_\nu \rangle = \frac{\langle E^* \rangle - \langle E_\gamma \rangle}{\langle B_N \rangle + \langle \mathrm{KE} \rangle}, \tag{30}$$

where $\langle E_\gamma \rangle$ is the mean gamma energy emitted per fragment, $\langle B_N \rangle$ is the mean neutron binding energy, and $\langle \mathrm{KE} \rangle$ is the mean kinetic energy of the prompt neutrons emitted. We performed systematic studies and found standard values for fission fragments which reproduce the

mean neutron evaporation to be $\langle E_\gamma \rangle = 4.0\,\mathrm{MeV}$ and $\langle B_N \rangle + \langle \mathrm{KE} \rangle = 6.5\,\mathrm{MeV}$. $\langle E^* \rangle$ is taken from eq. (7) for spontaneous fission and from eqs. (20) and (21) for fission following nuclear reactions. It is shown below that the above numbers fit quite well the value of the sawtooth curve for prompt neutrons. However, one should bear in mind that the nuclear structure may change rapidly with the fragment mass, and this will have an effect on the neutron evaporation. Therefore, eq. (30) should be taken to calculate mean values for neutron evaporation only. If neutron evaporation from single isotopes has to be known, a full statistical model calculation, for example PACE II, must be performed. We have done complete calculations for all mass splits for thermal-neutron–induced fission for different compound systems. These results will be presented elsewhere.

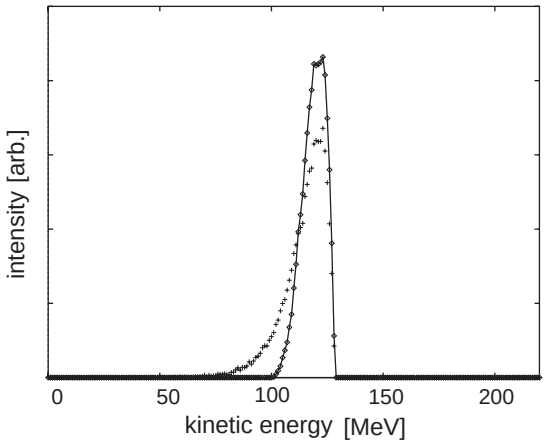

Fig. 2. Kinetic-energy distribution of a typical light fragment without and with inclusion of a cut-off parameter $c_s = 3$.

7 Variances and covariances

The variances of the excitation energy distributions are calculated to be

$$\sigma^2 = \frac{\int \Phi(x) \cdot (x - \langle x \rangle)^2}{\int \Phi(x)} \,. \tag{31}$$

This yields

$$\sigma^2_{E^*} = [a_{1,2} \cdot (\bar{f}Q)^2]^2 \,, \tag{32}$$

$$\sigma^2_{\mathrm{TXE}} = \frac{1}{2}(a_1 + a_2)^2 \cdot (\bar{f}Q)^4 \,, \tag{33}$$

and

$$\sigma^2_{\mathrm{TKE}} = \sigma^2_{\mathrm{TXE}} \,, \tag{34}$$

for spontaneous fission. If fission is induced by a nuclear reaction the variances change too. They can, however, be easily expressed by the mean values of the excitation energies

$$\sigma^2_{E^*_1} = (\langle E^*_1 \rangle)^2 \,, \tag{35}$$

$$\sigma^2_{E^*_2} = (\langle E^*_2 \rangle)^2 \,, \tag{36}$$

$$\sigma^2_{\mathrm{TXE}} = \frac{\langle \mathrm{TXE} \rangle^2}{2} \,, \tag{37}$$

$$\sigma^2_{\mathrm{TKE}} = \sigma^2_{\mathrm{TXE}} \,. \tag{38}$$

The covariance μ is defined as

$$\mu = \frac{1}{2}(\sigma^2_{E_1 *} + \sigma^2_{E_2 *} - \sigma^2_{\mathrm{TXE}}) \,. \tag{39}$$

Inserting eq. (32) and eq. (33) leads to a covariance of

$$\mu = (\bar{f}Q)^4 \cdot \frac{1}{4}(a_1 - a_2)^2 \,. \tag{40}$$

The covariance vanishes, whenever the level density parameter in the two fragments is equal, which is the case for symmetric mass and charge splits.

Calulations show that, in contrast to the results for the mean values of excitation and kinetic energies which do agree with experiment almost quantitatively, the variances are overestimated by a factor 2 to 3 when compared to experiment. This is a consequence of the use of exponential functions for fragment excitation which do not meet the requirement that the maximum possible excitation is limited to the Q-value of the reaction. We introduce therefore a cut-off parameter, which limits single-fragment excitation energy to a maximum value. We define the cut-off parameter c_s to be

$$E^*_{\mathrm{max}} = c_s \cdot \langle E^* \rangle \,. \tag{41}$$

Whereas the cut-off parameter has, for values $c_s \geq 2$, very little effect on the mean values, it drastically affects the variances of the distribution, and the lineshapes of the kinetic-energy distribution for the single fragment. Calculations with inclusion of the cut-off parameter are done using the Monte Carlo code, because it is not possible to give the analytical expressions for the distributions. Also in using the Monte Carlo code the pure independent distributions are used, which ensures that the covariance vanishes.

Figure 2 shows how, for a typical fission product in the light fission wing, the energy distributions of the fragment changes, if the cut-off parameter is applied. The distributions get much sharper, however the asymmetric lineshapes persist. This feature is observed usually on high-resolution mass spectrometers when scanning the energy distribution of a fragment, and will be subject of a forthcoming publication.

Figure 3 gives the dependence for mean kinetic energies and variances for the light and the heavy fragment as a function of the cut-off parameter for the reaction shown in fig. 1. Whereas the mean kinetic-energy values are only slightly affected by the introduction of the cut-off parameter, the variances of the distributions change drastically. Comparison with experiment shows that its value has to be about $c_s = 3.0$ to agree with the data. Also PACE II calulations show that with this cut-off parameter neutron evaporation, which is calculated from the distributions, is well reproduced [5]. A cut-off parameter of $c_s = 3.0$ discards high-energetic events corresponding to about 5% of

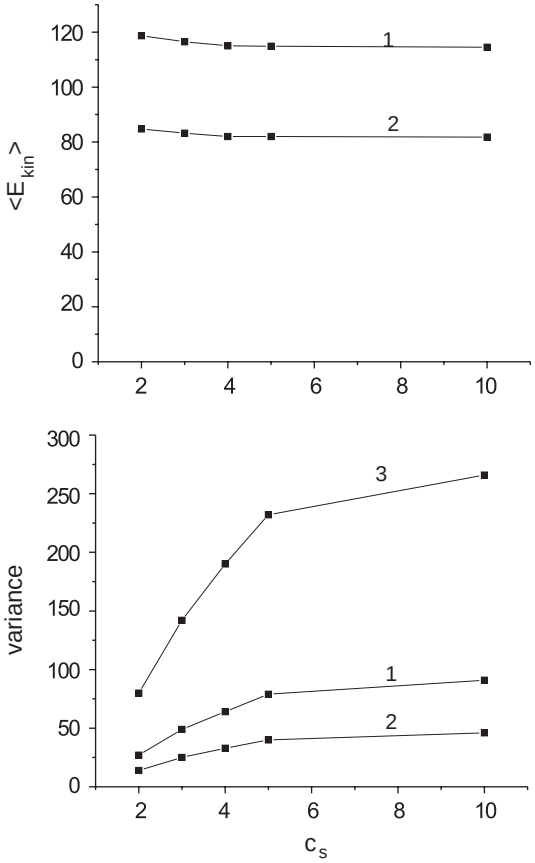

Fig. 3. Dependence of the value of the mean kinetic energy and the variance for the kinetic-energy distribution of the fragments on the cut-off parameter c_s. The numbers denote the light fragment (1) and the heavy fragment (2). Curve (3) gives the variance for the total kinetic energy. Parameters as given in fig. 1 were used.

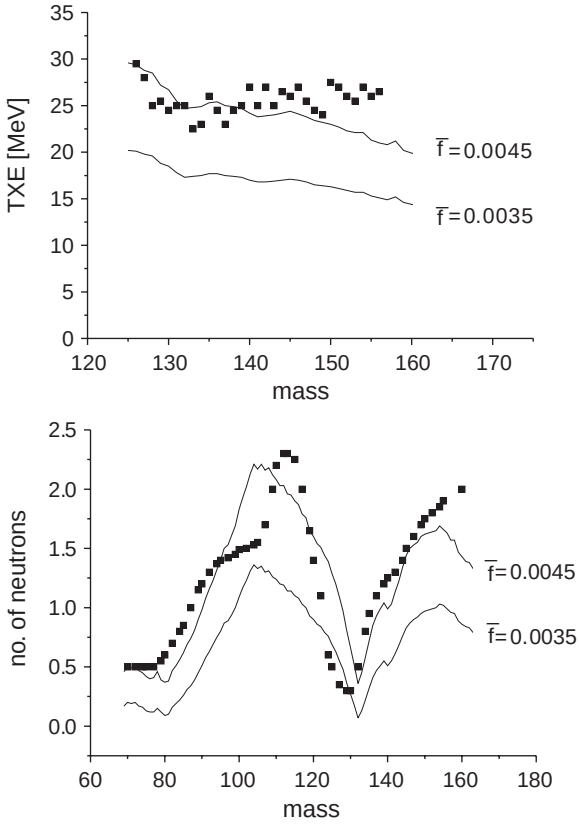

Fig. 4. ⟨TXE⟩-values (upper part) and neutron multiplicity (lower part) as a function of the fragment mass for ^{235}U(n, f). The calculations (solid lines) have been done for 2 different values of $\bar{f}$.

the total intensity, and limits the maximum value of TXE in spontaneous fission to about 60 MeV.

8 Results and discussion

In the present model there is only one global free parameter, $\bar{f}$, which determines the amount of excitation energy which is taken out of the Q-value. This parameter was fitted to ⟨TXE⟩-values from Lang *et al.* [6], for the thermal-neutron–induced fission of ^{235}U. The value for $\bar{f}$ was found to be

$$\bar{f} = 0.0045 \tag{42}$$

and is taken in the following to be independent of the mass split, the compound system, the reaction leading to fission, and the different fission paths which may be needed to account for the mass spectrum of a fissioning system.

It was found that the value of $\bar{f}$ is rather well fixed. In particular, besides mean excitation energies ⟨TXE⟩, the corresponding neutron evaporation values are also extremely sensitive to small changes in $\bar{f}$. This is exemplified in fig. 4, where different values of $\bar{f}$ were taken to fit the mean total excitation energy ⟨TXE⟩ and mean neutron evaporation, calculated for ^{235}U(n, f). A variation of about 20% was imposed on $\bar{f}$ to demonstrate its effect on the calculations. Experimental data for ⟨TXE⟩ from [6] are corrected for neutron evaporation. Neutron evaporation data have been taken from the compilation of Wahl [7].

Most of the structure in the ⟨TXE⟩ distribution, with which one initializes the calculations of the kinetic-energy distributions and the mean neutron evaporation, is imposed by the structure in the level density parameter as a function of the fragment mass. In particular the reduction of a for magic shell nuclei, and especially near doubly magic ^{132}Sn and ^{78}Ni, have drastic effects on the mean excitation of the single fragment.

If the compound nucleus allows for mass splits in two ($Z = 50$, $N = 82$) fragments, this effect is amplified, and ⟨TKE⟩-values may exhaust the available Q-value of the reaction. We show in fig. 5 the values of the level density parameter as function of the fragment mass as measured by Butz-Jørgensen and Knitter [8], and used in this work. In fig. 6 we show the result of the calculation of the mean excitation energy as a function of the fragment mass for the reactions ^{229}Th(n, f), ^{249}Cf(n, f) and ^{258}Fm(sf). Neutron multiplicity values $\langle M_\nu \rangle$ for the three systems are shown in the lower part of fig. 6. The similarity between the curves for the level density parameter, the mean

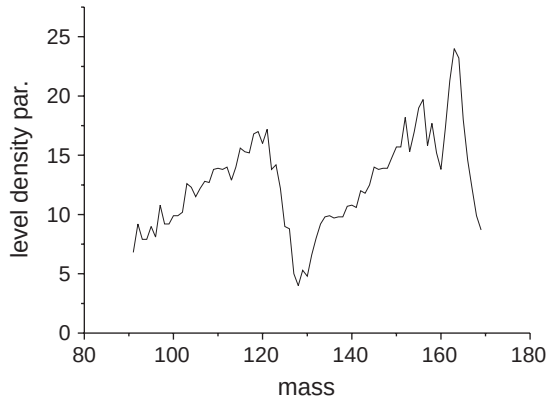

Fig. 5. Level density parameter as a function of fragment mass as used in the present calculations (taken from Butz-Jørgensen and Knitter [8]).

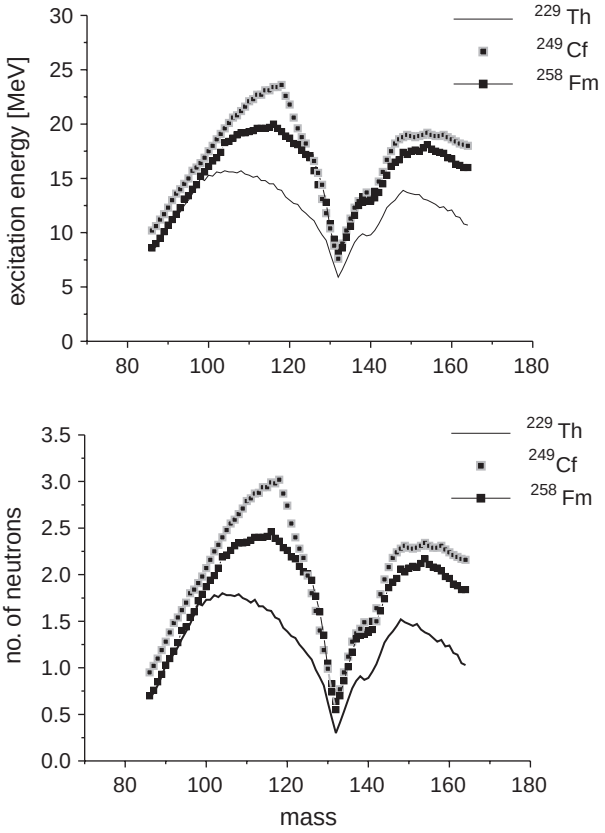

Fig. 6. Mean fragment excitation energy (upper part) and mean number of evaporated neutrons (lower part) calculated for the systems ^{229}Th(n,f), ^{249}Cf(n,f) and ^{258}Fm(sf).

excitation energy and the mean neutron evaporation as a function of the fragment mass is clearly recognisable.

The Q-value of the reaction counteracts the influence of the level density parameter insofar as in closed-shell regions, where the level density parameter is low, the Q-value tends to be high. However, the primary structure in the single-fragment excitation is strongly determined by the density of single-particle states in the fragments.

The excitation of fission products is independent of the appearance of fission modes, which may determine structures in the mass distribution. Also the mean values of excitation and kinetic energy, which are obtained by averaging over the mass or the nuclear charge are largely independent of a specific fission mode. Therefore, very general conclusions for fragment excitation in the actinide region can be drawn:

1. The probability of finding a single fragment with excitation close to zero is highest, as shown in fig. 1. However, the probability of finding both fragments simultaneously without excitation is zero, which means that true cold fragmentation into the ground states of the two fragments does not exist. On the other hand, the probability for very high excitation of the single fragment and the combined system is finite, so that in principle a considerable part of the Q-value can be converted to internal excitation, giving rise to high neutron evaporation values.
2. External excitation from a reaction cannot be converted into kinetic energy, but is always converted into heat, which increases the neutron evaporation probability.
3. The sawtooth aspect of the neutron evaporation curve with mass number stems from the structure of the level density parameter as a function of the mass. It has a universal character and is valid throughout the actinide region.
4. The mean single-fragment kinetic energy as a function of the fragment mass is almost constant for the light-wing masses, and strongly decreasing for masses in the heavy wing, see the following figures. This is a feature due mainly to kinematics which results from momentum and energy conservation in binary reactions.
5. Close to mass $A = 132$, single-fragment kinetic energies tend to increase due to reduced excitation. This is seen in general for all compound systems above thorium, where one ^{132}Sn fragment can easily be formed. Whenever two fragments can be formed with masses close to doubly magic ^{132}Sn, the total excitation energy will strongly decrease and the total kinetic energy will almost exhaust the Q-value of the reaction.

In fig. 7 we show the scatter plot for events from the Monte Carlo simulation, fig. 1, which have been sorted into the (E_1^*, E_2^*)-plane.

The lines connect locations of the same intensity. They are inclined to the E_1^*-axis with an angle of $\tan(\alpha) = \frac{a_1}{a_2}$.

From the picture it can be recognized, that a projection onto the E_1^*- or the E_2^*-axis individually yields the distribution function, eq. (1). If a window is set on the E_1^*- or E_2^*-axis, the projected image on the complementary axis always shows the same function, only the normalization changes. This means that any observable deduced from the internal excitation distribution stays the same, whatever condition is set on the complementary fragment. In particular this is valid for the sawtooth characteristics of the neutron evaporation curve.

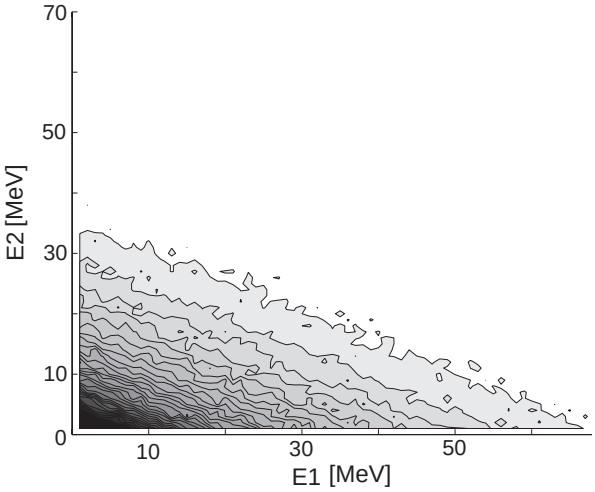

Fig. 7. Plot, where events of fig. 1 have been sorted into the (E_1^*, E_2^*)-plane. The lines connect locations of the same intensity.

In the following we will compare calculated values for $\langle \mathrm{TXE} \rangle$, $\langle \mathrm{TKE} \rangle$, $\langle E_{\mathrm{kin}} \rangle$ and mean neutron evaporation to experimental data. The calculations give primary quantities, before prompt neutron evaporation takes place. Measurements yield in general secondary quantities which refer to values after neutron evaporation. The neutron evaporation process has, however, only a small effect on kinetic energies. Each neutron takes away about 1% of the kinetic-energy value, which is of order 1 MeV, and in general only a small number of neutrons is evaporated. In few cases the neutron evaporation is accounted for in the data, and primary quantities are used. A comparison of experimental data with our calculations will be given for spontaneous fission of ^{252}Cf and ^{256,258}Fm, for thermal-neutron–induced fission in $^{229}\mathrm{Th}(n,f)$, $^{237}\mathrm{Np}(2n,f)$, and $^{239}\mathrm{Pu}(n,f)$, and for high energy fission of ^{219}Ac and ^{233}U. For these nuclei extensive experimental data exist.

In spontaneous fission excitation is due explicitly to the conversion of the Q-value into internal energy. Spontaneous fission of ^{252}Cf is well known, and in fig. 8 we compare the experimental data for $\langle E_{\mathrm{kin}} \rangle$ and $\langle \mathrm{TKE} \rangle$ from Schmitt *et al.* [9] and Mariolopoulos *et al.* [10] with the results of the calculations. Systematic features are well reproduced and the absolute values agree within a few per cent with the calculations.

For the fermium isotopes a rapid evolution of the mass spectrum was observed by Unik *et al.* [11], Hoffman *et al.* [12] and Hulet *et al.* [13], going along with strong variations of the total kinetic energy within a narrow mass range. Calculated $\langle \mathrm{TKE} \rangle$-values for spontaneous fission of ^{256}Fm and ^{258}Fm are shown in the lower part of fig. 9 as a function of mass. It appears that, despite the completely different mass spectra of both isotopes (^{256}Fm fission asymmetrically while ^{258}Fm has a strong symmetric fission component), the values of the total kinetic energies closely follow one another. This behavior is also seen for calculated $\langle \mathrm{TXE} \rangle$-values, upper part of fig. 9. In these heavy compound systems a charge split into two $Z = 50$

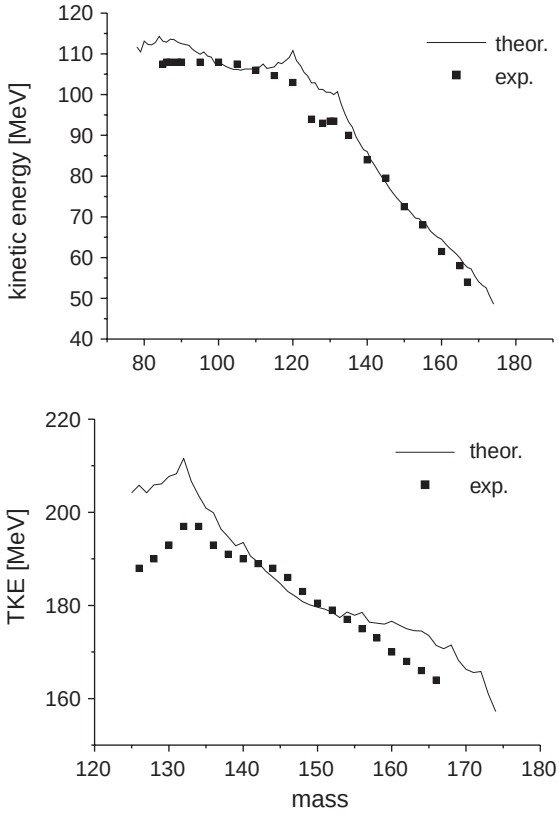

Fig. 8. Mean single-fragment kinetic energy and $\langle \mathrm{TKE} \rangle$-values for fragments from $^{252}\mathrm{Cf}(sf)$ as a function of the mass.

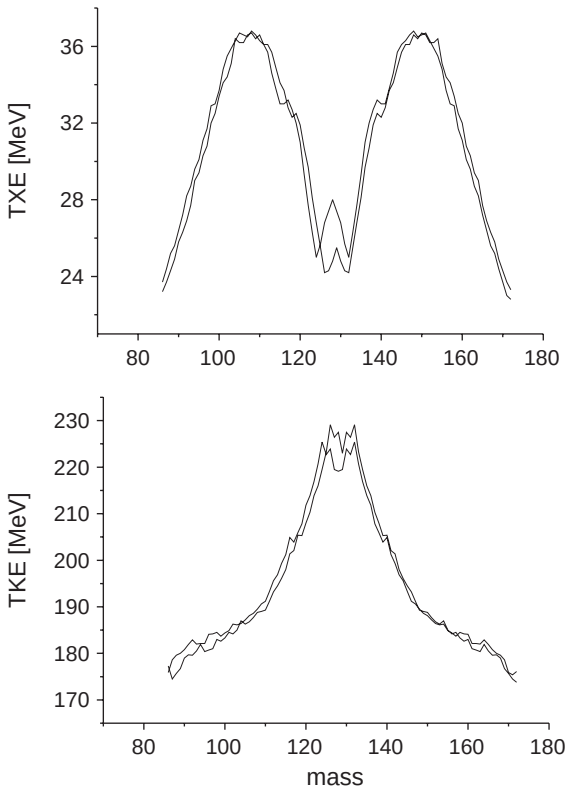

Fig. 9. Mean TXE- and TKE-values for the two systems $^{256}\mathrm{Fm}(sf)$ and $^{258}\mathrm{Fm}(sf)$.

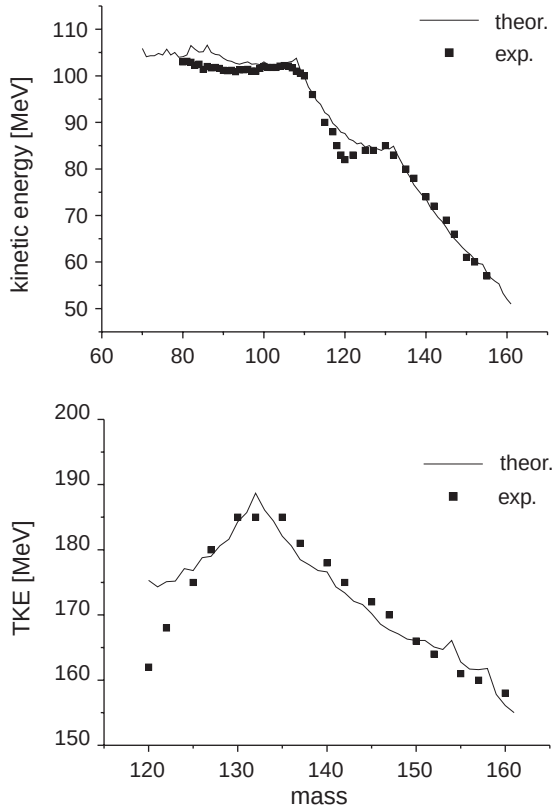

Fig. 10. Mean single-fragment kinetic energy and ⟨TKE⟩-values for fragments from ^{239}Pu(n, f) as function of mass.

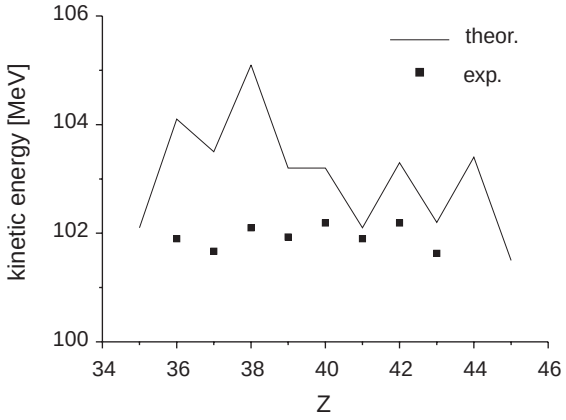

Fig. 11. Mean single-fragment kinetic-energy values for fragments from ^{239}Pu(n, f) as function of the nuclear charge.

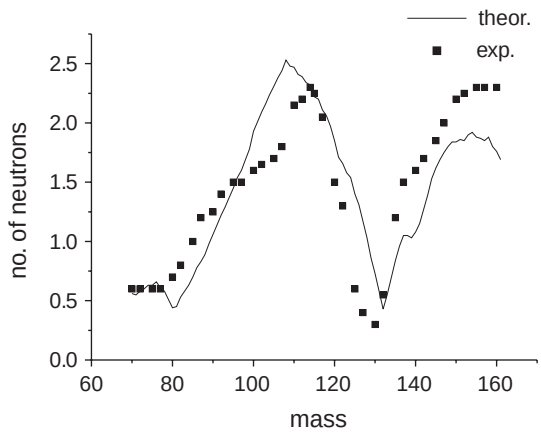

Fig. 12. Mean neutron evaporation values for ^{239}Pu(n, f).

isotopes is possible with neutron numbers near to $N = 82$, and the strongly reduced value of the level density parameter here leads to a small excitation probability. About 10 mass units away from symmetry, however, the ⟨TXE⟩-values increase by almost 13 MeV, leading to the observation of very different ⟨TKE⟩ for nearby masses. Whereas the mass spectra of both fermium isotopes strongly differ from each other, the energetics of the reaction is almost identical. The calculated values for ⟨TKE⟩ at mass $A = 130$ is about 225 MeV, whereas for mass $A = 120$-values of 205 MeV are obtained. These numbers are in agreement with the measured values of ⟨TKE⟩ = 230 MeV for mass $A = 130$ in ^{258}Fm(sf), and ⟨TKE⟩ = 205 MeV for mass $A = 120$ in both fermium systems.

In thermal-neutron–induced fission about 6 MeV is brought into the compound system due to the neutron binding energy of the captured neutron. This energy is shared between the fragments and increases $\langle E^*_{1,2}\rangle$ and ⟨TXE⟩-values. Extensive data for thermal-neutron–induced fission are known from experiments on the LOHENGRIN spectrometer in Grenoble. In particular fine structure on yield and energy distributions has been systematically investigated.

Figure 10 shows single-fragment kinetic energy and ⟨TKE⟩-values as a function of the fragment mass for ^{239}Pu(n, f). Experimental data are from Neiler *et al.* [14], and agree with the calculations to within a few per cent over the whole mass range form $A = 80$ to $A = 155$.

Fine structure on single-fragment kinetic energy comes about from the higher Q-value due to the pairing energy, when fragments with even neutron or proton number are formed. Most of the Q-value goes into kinetic energy, so that even fission fragments have higher energy than odd fragments. In the experiment this can be observed when the single-fragment kinetic energy is drawn as a function of the nuclear charge Z, because here any neutron evaporation does not spoil the effect, fig. 11. Experimental data are from Schmitt *et al.* [15], and it is seen in the figure that the odd even effect emerges. Calculated mean neutron evaporation for the Pu-system is shown in fig. 12 and compared to the data of Wahl [7]. It demonstrates that the ⟨TXE⟩-values are correctly calculated over the whole mass range from $A = 70$ to $A = 160$.

The lightest compound system accessible in thermal-neutron–induced fission is ^{230}Th. Single kinetic energy as a function of nuclear charge and mean total kinetic energies as a function of mass are shown in fig. 13. Experimental data are from Mariolopoulos *et al.* [10] for ⟨TKE⟩-values and from Djebara *et al.* [16] for single-fragment kinetic energies as a function of the nuclear charge. The data agree well with calculations, in particular the odd even effect is well reproduced. In fig. 14 we show as an example of

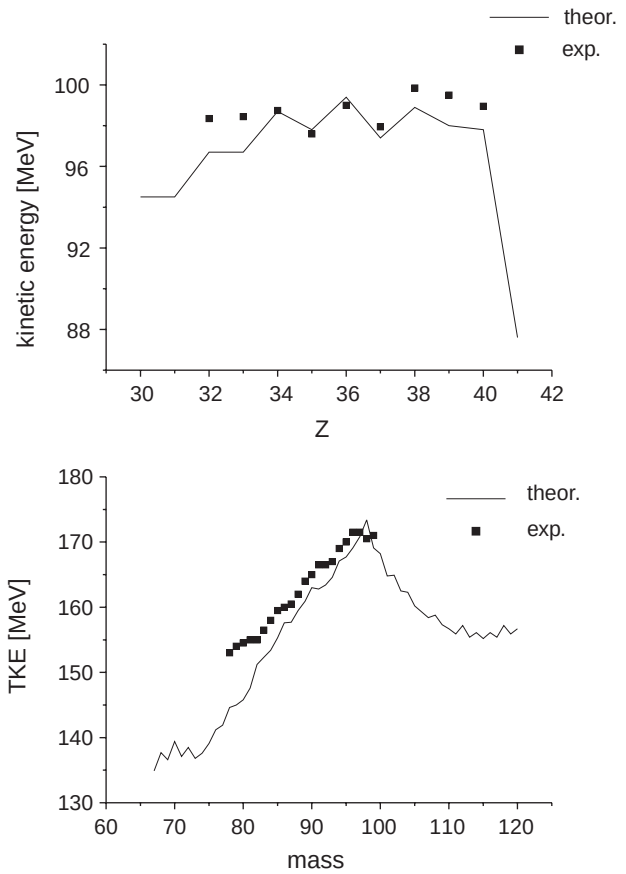

Fig. 13. Mean kinetic energies as function of the fragment charge and ⟨TKE⟩-values as a function of the fragment mass for ^{229}Th(n, f).

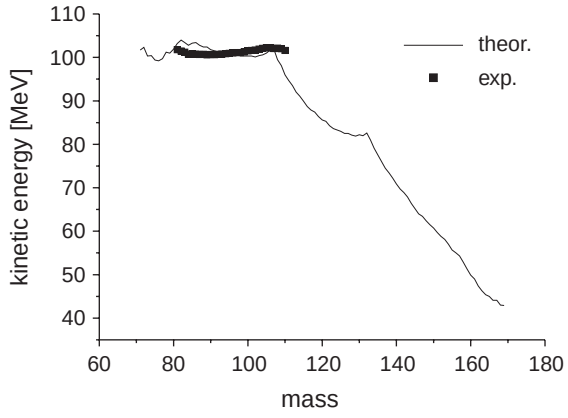

Fig. 14. Mean kinetic energies for ^{237}Np$(2n, f)$.

an odd-Z compound nucleus single-fragment mean kinetic energies for ^{237}Np$(2n, f)$. They are in agreement with the data from Martinez *et al.* [17].

Fission reactions as done at GSI, see Schmidt *et al.* [18], imply external excitation energies of about 12 MeV and produce compound systems below ^{238}U. In fig. 15 we show mean TKE-values for ^{233}U and ^{219}Ac measured as a function of the fragment charge Z. The calculations reproduce fully the measured data within the range

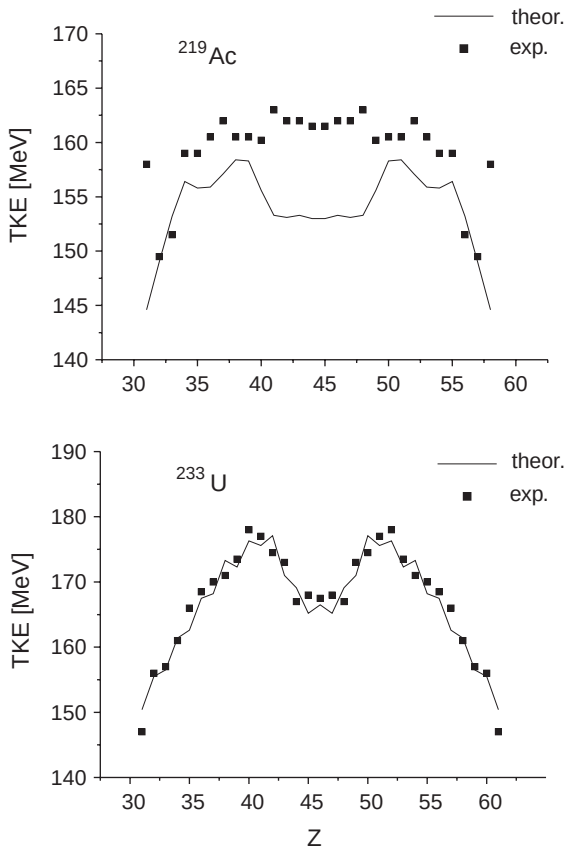

Fig. 15. ⟨TKE⟩-values for ^{233}U and ^{219}Ac as measured at GSI and compared to the calculations.

from $Z = 30$ to $Z = 60$ for ^{233}U. Also for the very light system ^{219}Ac a good agreement with the data with maximum 5% deviation is seen, and in particular the quite flat behaviour over a wide range of fragment charges and the strong decrease at the edges of the distribution are well reproduced.

9 Conclusions

We have shown that a statistical model with one global free parameter is able to reproduce mean values of fragment excitation and fragment kinetic energy for compound systems from ^{219}Ac to ^{258}Fm to a high degree of accuracy. Calculations agree with experimental data over the whole range of fission product mass from $A = 70$ to $A = 160$ almost quantitatively. It was also shown that external excitation energy brought into the compound system is correctly taken into account in the model. Details of kinetic-energy distributions as well as global features are reproduced, and in particular the model gives correct results in regions of rapidly changing mass spectra around fermium. By cutting off the exponential function for single-fragment excitation at higher energies not only the mean but also higher moments of the kinetic-energy distribution of the single fragment are reproduced.

The basic assumption of the model was a function for the single-fragment excitation which depends on the level density parameter and the reaction Q-value. The density distribution for fragment excitation follows an exponential behavior. The combined system near the scission point has an excitation distribution resulting from almost independent fragment excitation. From this TXE distribution the TKE distribution is derived, and furthermore the kinetic-energy distributions of the fragments are calculated. The success of the model demonstrates that fragment excitation is a universal behavior for all fissioning systems, and is independent of the mass distribution and the nuclear reaction leading to fission. Excitation in nuclear fission is therefore completely decoupled from the distribution of mass and charge yield, and independent from possible fission modes which may cause the structures in yield which are observed.

Finally, it turns out that excitation of fission fragments is likely to be one of the cleanest reactions known in nuclear physics of heavy systems. One global parameter is needed to reproduce the wealth of experimental data in the transactinide region.

References

1. A.H. Wapstra, G. Audi, R. Hoekstra, At. Data Nucl. Data Tables **39**, no. 2, 281 (1988).
2. P. Möller, J.R. Nix, At. Data Nucl. Data Tables **39**, no. 2, 213 (1988).
3. *Handbook of Chemistry and Physics*, 55th edition (CRC Press, 1974).
4. P.M. Stwertka, T.M. Cormier, M. Herman, N.G. Nicolis, Phys. Lett. B **150**, 91 (1985).
5. H.R. Faust, Z. Bao, to be published in Nucl. Phys. A.
6. W. Lang, H.G. Clerc, H. Wohlfarth, H. Schrader, K.H. Schmidt, Nucl. Phys. A **345**, 34 (1980).
7. A.C. Wahl, At. Data Nucl. Data Tables **39**, 1 (1988).
8. C. Butz-Jørgensen, K.H. Knitter, Nucl. Phys. A **490**, 307 (1988).
9. H.W. Schmitt, J.H. Neiler, F.J. Walter, Phys. Rev. **141**, 1146 (1966).
10. G. Mariolopoulos, Ch. Hamelin, J. Blachot, J.P. Bocquet, R. Brissot, J. Crançon, H. Nifenecker, Ch. Ristori, Nucl. Phys. A **361**, 213 (1981).
11. J.P. Unik, J.E. Gindler, L.E. Glendenin, K.F. Flynn, A. Gorski, R.K. Sjoblom, in *Proceedings of the Third International Atomic Energy Agency Symposium on the Physics and Chemistry of Fission, Rochester, 1973*, Vol. **II** (International Atomic Energy Agency, Vienna, 1974) p. 19.
12. D.C. Hoffman, J.B. Wilhelmy, J. Weber, W.R. Daniels, E.K. Hulet, R.W. Lougheed, J.H. Landrum, J.F. Wild, R.J. Dupzyk, Phys. Rev. C **21** 972 (1980).
13. E.K. Hulet, J.F. Wild, R.J. Dougan, R.W. Lougheed, J.H. Landrum, A.D. Dougan, P.A. Baisden, C.M. Henderson, R.J. Dupzyk, R.L. Hahn, M. Schädel, K. Sümmerer, G.R. Bethune, Phys. Rev. C **40** 770 (1989).
14. J.H. Neiler, F.J. Walter, H.W. Schmitt, Phys. Rev. **149**, 894 (1966).
15. C. Schmitt, A. Gessous, J.P. Bocquet, H.G. Clerc, R. Brissot, D. Engelhardt, H.R. Faust, F. Gönnenwein, M. Mutterer, H. Nifenecker, J. Pannicke, Ch. Ristori, J.P. Theobald, Nucl. Phys. A **430**, 21 (1984).
16. M. Djebara, M. Ashgar, J.P. Bocquet, R. Brissot, M. Maurel, H. Nifenecker, Ch. Ristori, Nucl. Phys. A **425**, 120 (1984).
17. G. Martinez, G. Barreau, A. Sicre, T.P. Doan, P. Audouard, B. Leroux, W. Arafa, R. Brissot, J.P. Bocquet, H.R. Faust, P. Koczon, M. Mutterer, F. Gönnenwein, M. Asghar, U. Quade, K. Rudolph, D. Engelhardt, E. Peasecki, Nucl. Phys. A **515**, 433 (1990).
18. K.H. Schmidt, S. Steinhäuser, C. Böckstiegel, A. Grewe, A. Heinz, A.R. Junghans, J. Benlliure, H.G. Clerc, de M. Jong, J. Müller, M. Pfützner, B. Voss, Nucl. Phys. A **665**, 221 (2000).